Chemical Physics Letters 692 (2018) 395–401

Contents lists available at ScienceDirect

Chemical Physics Letters

journal homepage: www.elsevier.com/locate/cplett

Research paper

Two-color resonance enhanced multi-photon ionization and mass analyzed threshold ionization spectroscopy of 2-aminobenzonitrile and the CN substitution effect

Yinghui Jin, Yan Zhao, Yonggang Yang, Lirong Wang, Changyong Li *, Suotang Jia

State Key Laboratory of Quantum Optics and Quantum Optic Devices, Institute of Laser Spectroscopy, Shanxi University, Taiyuan, Shanxi 030006, China
Collaborative Innovation Center of Extreme Optics, Shanxi University, Taiyuan, Shanxi 030006, China

ARTICLE INFO

Article history:
Received 17 October 2017
In final form 28 December 2017
Available online 29 December 2017

Keywords:
Two-color resonance enhanced multi-photon ionization
Photo ionization efficiency
Mass-analyzed threshold ionization
2-Aminobenzonitrile
Vibronic spectrum
Cation spectrum

ABSTRACT

Two-color resonance two-photon ionization and mass analyzed threshold ionization spectra of 2-aminobenzonitrile have been obtained. The band origin of the $S_1 \leftarrow S_0$ transition and the precise ionization energy (IE) were determined to be 31,265 ± 2 cm^{-1} and 66,653 ± 5 cm^{-1}, respectively. The most active modes in the S_1 and D_0 states are related to the in-plane ring vibrations. The relative errors of IE estimated by CBS-QB3 and G4 are −0.18% and +1.47%, respectively. The theoretical calculations well support our experimental findings.

© 2017 Elsevier B.V. All rights reserved.

1. Introduction

2-, 3-, and 4-aminobenzonitrile (2ABN, 3ABN, 4ABN) are usually used as pharmaceutical intermediates. The properties of 4ABN cation had been investigated by Tzeng group [1] with MATI technique and Sakota, etc. [2] with ZEKE spectroscopy. The vibrational spectra of 2ABN in the neutral ground state S_0 and the excited state S_1 have been reported by several groups. Najbar's group investigated the laser induced fluorescence (LIF) excitation spectra of 2ABN and 3ABN theoretically and experimentally [3], and reported the spectral assignments in the S_0 and S_1 states. To the best of our knowledge, detailed information about the ionization energy, the cationic spectra of 2ABN has never been studied. In this paper, two-color resonance enhanced multi-photon ionization (2-C REMPI) and mass analyzed threshold ionization spectra of 2ABN are presented. Density function theory (DFT) calculations for the S_0, S_1, and D_0 states are performed. According to the calculated results, the spectra in S_1 and D_0 states are assigned by the method of Varsanyi and Szoke [4,5]. The theoretical calculations provide satisfactory explanations for the experimental findings.

2. Experimental and computational details

2.1. Experimental method

The experimental system is similar to Refs. [6–8]. A linear time-of-flight mass spectrometer was used. Two turbo molecular pumps (FF-200/1300) with a mechanical pump (RVP-12, 14l/s) as a fore-line pump were used to exhaust. The working pressures were $\sim 6 \times 10^{-4}$ Pa in beam source and $\sim 2 \times 10^{-6}$ Pa in ionization house. The sample of 2ABN (98% purity) was purchased from Energy Chemical Corporation and used without further purification. The solid sample was heated to about 120 °C to obtain sufficient vapor pressure, seeded into 2 bar of Ar and expanded into the vacuum though a General Valve with 0.8 mm diameter orifice. The molecular beam was collimated by a skimmer (1-mm-diam aperture) located 12 mm downstream from the nozzle orifice. The ion free flight distance was ~48 cm. A dual-stacked microchannel plate (Shanxi Changcheng Microlight Equipment Co., 25 mm diameter) was used to detect the ion signal.

Two independent tunable UV laser systems were controlled by a pulse delay generator (DG645 with 8 delay outputs). The first dye laser (Sirah CBR-D-24) was pumped by a pulsed frequency-doubled Nd:YAG laser (Indi-40-10). The visible radiation was frequency-doubled using a frequency conversion unit (SHG-280). The second dye laser (Sirah PrecisionScan-D with two 90 mm

* Corresponding author.
E-mail address: lichyong@sxu.edu.cn (C. Li).

https://doi.org/10.1016/j.cplett.2017.12.073
0009-2614/© 2017 Elsevier B.V. All rights reserved.

gratings of 1800 l/mm and 3000 l/mm) was pumped by another pulsed frequency-tripled Nd:YAG laser (Q-smart 850). Its output was frequency-doubled using an autotracking frequency doubling unit (WS-auto, SHG-250). In REMPI experiment, we fixed the ionization laser wavelength to 282 nm and scanned the excitation laser wavelength. A wavemeter (HighFinesse WS-7) was used to calibrate the wavelengths of these two dye lasers.

In the MATI experiments, about 0.1 μs after the occurrence of the laser pulses, a pulsed electric field of −1.07 V/cm (duration = 15 μs) was switched on to reject the prompt ions. After a time delay of about 21.0 μs, a second pulsed electric field of +143 V/cm (duration = 50 μs) was applied to field-ionize the Rydberg neutrals. The ion signal was collected and analyzed by a multichannel scaler (SR430), and then transferred to a computer. Mass spectra were accumulated for 300 laser shots at every scanning step (0.02 nm or ~1.3 cm^{-1}). Composite optical spectra of intensity versus wavelength were then constructed from the individual mass spectra.

2.2. Computational method

All the calculations are performed using the GAUSSIAN 09 program package [9]. For the excited state S_1, TD-B3LYP/6311++G(d,p) method was used, whereas for the natural ground state S_0 and the cation ground state D_0, B3PW91/6311++G(d,p) method was employed. The calculated vibrational frequencies were scaled by a factor (see Tables 1 and 2) to correct approximately for the combined errors, which stem from basis set incompleteness and negligence of vibrational anharmonicity and electron correlation. In order to more accurately estimate the ionization energy (IE), we also performed CBS-QB3 and G4 calculations for S_0 and D_0 states. The IE was obtained as the difference between the ground state energies of the cation and the corresponding neutral.

3. Results

3.1. Two-color REMPI spectra

Fig. 1 shows the two-color REMPI spectra of the 2-aminobenzonitrile. The band origin of $S_1 \leftarrow S_0$ electronic transition appears at 31,265 cm^{-1}. More than thirty vibrational bands are found. The experimental and calculated vibration frequencies are listed in Table 1. The results from the Ref. [3] are also listed in Table 1 for comparison.

Table 1
Assignment of the observed bands (cm^{-1}) in the 2C-REMPI spectra of the 2-aminobenzonitrile[a].

Ref. [3]	This work[a]			Assignment and approximate description[b]
Exp.	Exp.	Exp. Rel. Int.	Cal.	
140.2	139.4	78	146.0	βCN
183.1	182.9	27	187.5	$10b_0^1$,γCH,γC-NH_2
272.2	272.2	17	249.3	$10a_0^1$, γCH
	280.1	45		β CN_0^2
	321.9	18		$10b_0^1$ βCN
342				
371	369.9	81	365.3	15_0^1,βCN, βNH_2
429.9	422.0	22		βCN_0^3
443.9	442.1	100	439.9	$6b_0^1$, βCCC
499.9	508.6	48		15_0^1 βCN
518	516.7	52	522.4	$6a_0^1$, βCCC
	583.5	82	584.9	$9b_0^1$, βCN
	624.1	23	625.6	11_0^1, γCH
	648.6	23		15_0^1 β CN_0^2
	656.7	28		$6a_0^1$ βCN_0^1
684	681.2	54	681.2	1_0^1, breathing
	724.1	52	730.6	$17b_0^1$, γCH
	740.5	27		15_0^2
	812.4	49		15_0^1 $6b_0^1$
	822.6	28		1_0^1 βCN_0^1
	830.9	43	826.8	12_0^1, βCCC
841	839.1	28		$6b_0^1$ βCN_0^2
	866.0	20		$10b_0^1$ 1_0^1
	884.6	64	879.2	5_0^1, γCH
	952.9	51		15_0^1 9b
	959.1	39		1_0^1 β CN_0^2
	971.6	31	963.7	βNH_2
1005.8	1002.8	46	1007.4	$18b_0^1$, βCH
1013.7	1011.1	27		βCN_0^2 15_0^2
	1025.9	49		$6b_0^1$ $9b_0^1$
	1052.9	32	1068.0	15_0^1 1_0^1
	1090.5	32	1074.8	$18a_0^1$, βCH
	1124.0	29	1117.0	$6b_0^1$ 1_0^1
	1142.9	30	1158.7	13_0^1, βCCC
	1164.0	24		$17b_0^1$ $6b_0^1$
	1185.0	32	1239.1	$7a_0^1$, νC-NH_2

[a] The experimental values are shifts from 31 265 cm^{-1}, whereas the calculated values are obtained from the TD-B3LYP/6-311++G** calculations, scaled by 0.9702. Exp. Rel. Int. represent the experimental values with respect to the measured $6b_0^1$ band intensity.
[b] ν, stretching; β, in-plane bending; γ, out-of-plane bending.

Table 2
Assignment of the observed bands (in cm^{-1}) in the MATI spectra of 2-aminobenzonitrile[a]

Intermediate level in the S_1 state					Cal.	Assignment and approximate description[b]
0	βCN	15	6b	1		
116					114	γCN
	134			134	139	βCN^1
	253					βCN^2
344					348	$10a^1$, γCCC
		380			369	15^1, βNH_2
446					440	$16b^1$, γCCC
			450		446	$6b^1$, βCCC
	476					$\beta CN^1 10a^1$
		498			500	$16a^1$, γCCC
539					536	$6a^1$, βCCC
	575	571				$\beta CN^1 16b^1$
580					583	γNH_2 twisting
		594			586	$9b^1$, βCN
	622					$\beta CN^1 16a^1$
702			704	704	702	1^1,breathing
					709	4^1, γCCC
	717					$\beta CN\ ^1\gamma NH_2$
		724				$15^1 10a^1$
786			786		771	11^1,γCH
		824				$15^1 16b^1$
				838	838	12^1,βCCC
	834					$\beta CN\ ^1 1^1$
846						$\beta CN\ ^2\gamma NH_2$
		867			866	$17a^1$,γCH
			894			$6b^1 16b^1$ or $6b^2$
			937			$10a^1 9b$
	957	961			964	$17b^1$, γCH
	983		986		986	5^1, γCH
991					999	βNH_2
1020					1017	$18b^1$βCH
	1028		1028			$6b^1\gamma NH_2$
				1048		$10a^1 1^1$
		1085				$15^1 1^1$
1127					1129	$18a^1$, βCH
			1152	1151		$6b^1 1^1$
	1154					$\beta CN\ ^1 18b^1$
1161		1161			1166	$9a^1$, βCH
			1171		1183	13^1, νC-CN
		1224				$17a^1 15^1$
			1233			$11^1 6b^1$
	1266					$\beta CN\ ^2 18b^1$
1279				1278		$1^1\gamma NH_2$
1293	1293		1296		1290	3^1,βCH
	1301					$17b^1 10a^1$
			1341			$6b^2 16b^1$ or $6b^3$
1355					1362	14^1, βCCC
1376					1370	$7a^1$, νC-NH_2
	1402	1401		1402		1^2
				1412		4^2
	1429				1457	$19a^1$, νCC
1471						$18a^1 10a^1$
			1476	1475	1473	$19b^1$, βCCC
		1504				$15^1 18a^1$
	1510				1508	$8a^1$, βCCC
		1539				$15^1 9a^1$
	1545			1549		$12^1 1^1$
1580	1583		1582		1589	$8b^1$, βCCC
	1608				1637	βNH_2, scissoring
		1673				$15^1 3^1$
	1714					$8b^1\beta CN\ ^1$

[a] The experimental values are shifts from 66,653 cm^{-1}, whereas the calculated ones are obtained by the B3PW91/6311++G(d,p) level of calculations, scaled by 0.9788.
[b] Assignments are based on Varsanyi's nomenclature. ν, β, and γ represent stretching, in-plane bending, and out-of-plane bending, respectively.

The DFT calculations show that 2-aminobenzonitrile belongs to C_1 point group in the S_0 state and C_s point group in the S_1 state. Electron redistribution during the $\pi^* \leftarrow \pi$ electronic excitation causes a strong interaction between the aromatic ring and the amino group and a significant change in molecular geometry, as discussed in Section 4.1. Spectral features are assigned base on our calculations and conformity with the available data on substituted anilines. Vibronic transitions are expressed in the Wilson notation based on benzene modes, where the $v' \leftarrow v''$ transition in the normal mode n is represented by $n^{v'}_{v''}$ [10].

Vibronic transitions involving the in-plane ring deformation are usually active for substituted anilines [11–14]. The intense bands at 369.9, 442.1, 516.7, 583.5, 830.9, and 1002.8 cm^{-1} are assigned to transitions 15^1_0, $6b^1_0$, $6a^1_0$, $9b^1_0$, 12^1_0, and $18b^1_0$, respectively. These bands belong to in-plane bending of the ring. The weak bands at 1090.5 and 1142.9 cm^{-1} are assigned to transitions $18a^1_0$ and 13^1_0,

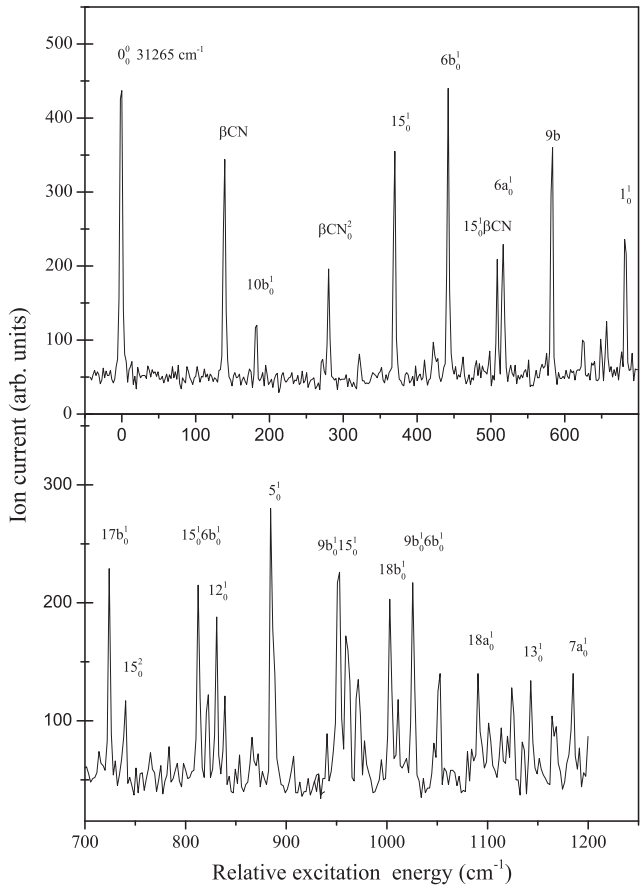

Fig. 1. Two color REMPI spectrum of 2-aminobenzonitrile obtained by fixing the ionization laser wavelength to 282 nm and scanning the excited laser wavelength.

respectively, which also belong to in-plane bending of the ring. Modes 1 and 7a represent the breathing and substituent-sensitive C-NH_2 in-plane stretching vibrations, respectively, and the corresponding transitions 1^1_0 and $7a^1_0$ are located at 681.2 and 1185.0 cm^{-1}, respectively. Ring out-of-plane modes 10b, 10a, 11, 17b, and 5 are also observed. The intense bands $17b^1_0$, 5^1_0, and weak bands $10b^1_0$, $10a^1_0$, 11^1_0 are located at 724.1, 884.6 182.9, 272.2, and 624.1 cm^{-1}, respectively. CN in-plane bending βCN is located at 139.4 cm^{-1}, and NH_2 in-plane rocking is located at 971.6 cm^{-1}. The other spectral features in the Fig. 1 are assigned to the combinations or overtones of experimentally observed several intense modes.

3.2. Photo ionization efficiency spectrum

Fig. 2 displays the PIE curve, recorded via the $S_1 0^0$ (31,265 cm^{-1}) intermediate state. A step corresponding to the ionization threshold of 2-aminobenzonitrile is clearly seen at a total photon energy of 66,654 ± 10 cm^{-1}. The G4 calculations yield the value of 66,967 cm^{-1} for the ionization energy, which is larger than the measured one by 313 cm^{-1}. And the CBS-QB3 calculation yields the value of 66,533 cm^{-1}, which is lower than the measured one by 121 cm^{-1}. So, the relative errors of G4 and CBS-QB3 calculations are +0.47% and −0.18% for 2ABN, respectively. This indicates that the methods of G4 and CBS-QB3 are sufficient to help selecting the appropriate dye for the ionization laser.

3.3. Threshold ion spectra

Figs. 3 and 4 show the threshold ion spectra, recorded via the 0^0 vibrationless and the βCN, 15^1, $6b^1$, and 1^1 vibrational levels in the

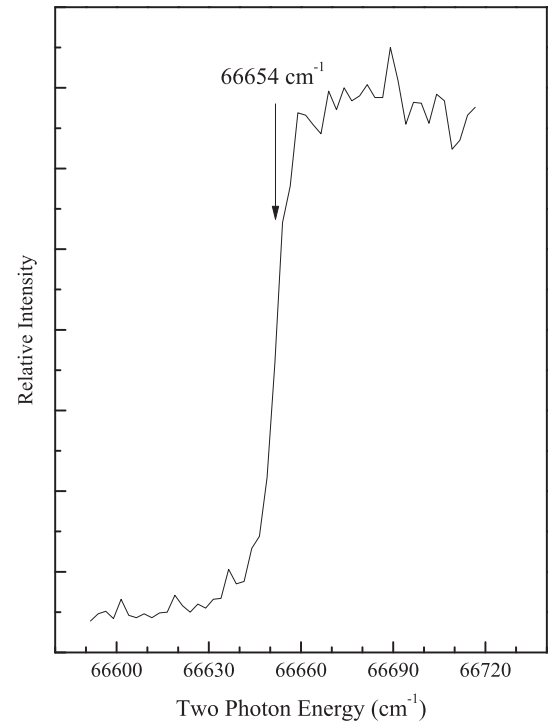

Fig. 2. Photoionization efficiency spectrum of *2*-aminobenzonitrile via $S_1 0^0$.

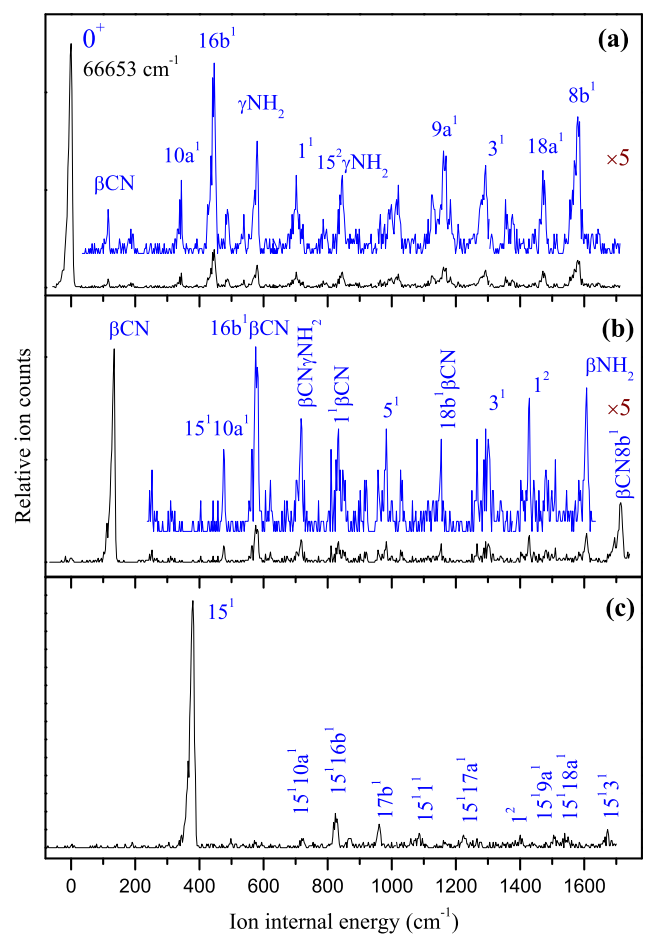

Fig. 3. Threshold ionization spectra of *2*-aminobenzonitrile by MATI method via the (a) $S_1 0^0$, (b) S_1βCN, (c) $S_1 15^1$ intermediate states.

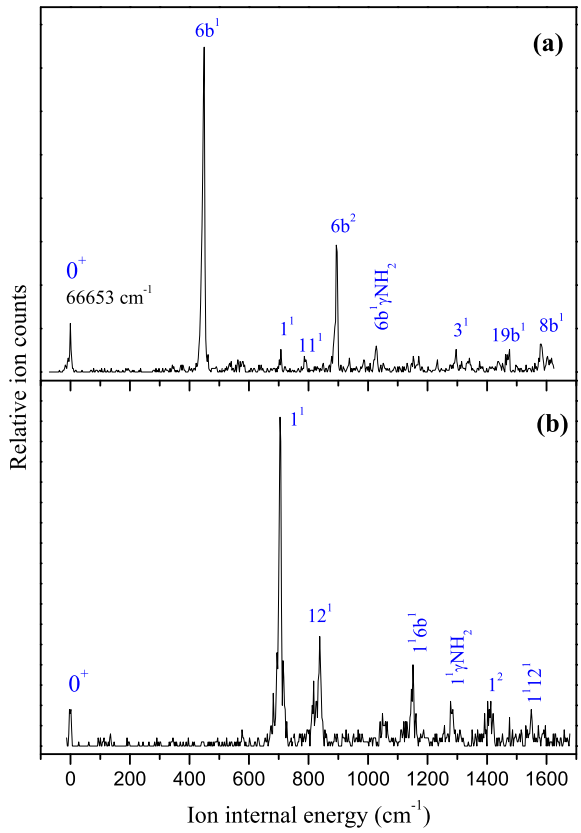

Fig. 4. Threshold ion spectra of *2*-aminobenzonitrile by MATI method via the (a) $S_1 6b^0$, (b) $S_1 1^1$ intermediate states.

S_1 state of 2-aminobenzonitrile. Since MATI spectroscopy involves ionization of molecules in the high Rydberg states by a delayed electric field pulse, the energy shift due to the Stark effect may be approximated to be $4.0F^{1/2}$.[27] Analysis of the 0^+ bands gives the field-corrected adiabatic IE of 66 653 ± 5 cm^{-1}, which is in excellent agreement with that determined by our PIE experiments.

Table 2 lists the frequencies of the observed MATI bands with the corresponding calculated values and their assignments. When $S_1 0^0$ is used as the intermediate level, the band origin 0^+ related to ion ground state appears to be the most intense peak in the MATI spectrum, as shown in Fig. 3a. The similar trends can be seen in Figs. 3 and 4 when S_1βCN, $S_1 15^1$, $S_1 6b^1$, and $S_1 1^1$ are used as the intermediate levels. This indicates that the geometry of the cation resembles that of the neutral molecule in the S_1 state. The spectral assignment was mainly based on the B3PW91/6311++g(d,p) calculations and conformity with the experimental data in the S_1 states, as listed in Table 2. The bands at 380, 594, 1127, 1161, 1293, 1355, 1429, 1475, 1510, 1580 cm^{-1} are assigned to in-plane ring deformations 15^1, $9b^1$, $18a^1$, $9a^1$, 3^1, 14^1, $19a^1$, $19b^1$, $8a^1$, $8b^1$, respectively. The MATI bands at 450, 539, 703, 838, 1171, 1376 cm^{-1} are caused by in-plane ring stretching $6b^1$, $6a^1$, 1^1, 12^1, 13^1, $7a^1$, respectively. The spectral features appear at 344, 446, 498, 707, 786, 867, 959, 983 cm^{-1} are assigned to out-of-plane ring vibrations $10a^1$, $16b^1$, $16a^1$, 4^1, 11^1, $17a^1$, $17b^1$, 5^1, respectively. The CN out-of-plane motion is located at 116 cm^{-1}, and its in-plane bending at 134 cm^{-1}. The NH_2 out-of-plane twisting, in-plane rocking and scissoring vibrations appear at 580, 991, and 1608, respectively. Other bands are assigned to the combinations or overtones of several intense normal modes, see Table 2.

4. Discussion

4.1. Molecular structure

In general, the amino group is out of the aromatic ring plane in the natural ground state S_0, and in the ring plane for the S_1 and D_0 states. Our density function theory calculations are in agreement with this rule. However, in the S_0 state of 2-aminobenzonitrile, the angle of the amino group with respect to the plane of the aromatic ring is about 17°, which is much less than ~40° of aniline [15], diaminobenzene [16], 4-aminobenzonitrile [1,2], and methylaniline [17]. This is probably duo to by the intramolecular hydrogen bond. Kim's group reported the intramolecular hydrogen bond in 2-aminopyridine [18], which leads to the amino group angle with respect to the plane of the ring less than 30°.

Table 3
Measured electronic transition and ionization energies, and calculated HOMO, LUMO energies of CN, F, OCH_3, CH_3, OH substituted aniline, phenol, and anisole (unit: cm^{-1})[a].

Molecule	Measured						Calculated		
	E_1	ΔE_1	E_2	ΔE_2	IE	ΔIE	LUMO	HOMO	Gap
Aniline[b]	34,029	0	28,242	0	62,271	0	−2713	−46,831	44,119
2-aminobenzonitrile[c]	31,265	−2764	35,388	7146	66,653	4382	−12,690	−51,559	38,869
p-cyanoaniline[d]	33,481	−548	33,012	4770	66,493	4222	−10,313	−51,638	41,325
2-hydroxyaniline[e]	33,442	−587					−1956	−44,861	42,905
2-Methoxyaniline[f]	33,875	−154	24,803	−3439	58,678	−3593	−821	−44,007	43,186
2-Methylaniline [g]	34,318	289	26,684	−1558	61,002	−1269	−1800	−46,081	44,281
2-Fluoroaniline[h]	34,583	554	29,061	819	63,644	1373	−3948	−48,383	44,435
Phenol[i]	36,349	0	32,276	0	68,625	0	−4422	−51,767	47,345
4-cyanophenol[j]	35,548	−801	37,150	4874	72,698	4073	−12,479	−56,765	44,286
Anisole[k]	36,383	0	30,016	0	66,399	0	−3575	−50,521	46,946
4-cyanoanisole[A,c]	35,549	−834	34,860	4844	70,409	4010	−11,843	−55,382	43,539

[a] E_1: ($S_1 \leftarrow S_0$), E_2: ($D_0 \leftarrow S_1$), Gap: LUMO − HOMO.
[b] Refs. [21,22].
[c] This work.
[d] Ref. [1].
[e] Ref. [27].
[f] Ref. [26].
[g] Ref. [17].
[h] Ref. [25].
[i] Ref. [23].
[j] Ref. [28].
[k] Ref. [24].
[A] Ref. [6].

Table 4
The several intense vibrations in the S_1 and D_0 states of 2-aminobenzonitrile (cm^{-1}).

	in-plane					out-of-plane ring bending	
	rocking	ring deformation	ring stretching				
	βCN	15	6b	1	12	17b	5
S_1	139	370	442	681	831	724	885
D_0	134	380	450	704	838	961	986

4.2. Transition energy, IE and substituent effect

The substitution of a functional group on an aromatic ring can lower the zero-point energy (ZPE) level of an electronic state. The degree of the lowing reflects the intensity of the interaction between the substituent and the ring. If the extent of the lowering of the ZPE level of the upper electronic state is greater than that of the lower one, it generates a red shift in the transition energy. Oppositely, it gives rise to a blue shift [19,20].

Table 3 lists the measured transition energies and adiabatic IEs of aniline [21,22], phenol [23], anisole [24], and their CN substitutes by REMPI, ZEKE, or MATI spectroscopy [1,6,17,25–28]. It can be seen that substitutions of OCH_3, OH, and CN all lower the excited energy E_1. This indicates that the interaction of the substituent and the ring in the upper electronic state is stronger than in the lower one. Specially, CN substituent makes a much larger lowering in excitation energy than the others, which means that CN group has a much larger interaction with the ring in the excited state than in the ground state. The CH_3 and F substitutions slightly increase the excitation energy E_1, indicating that the interaction between the substituent and the ring is weaker in the S_1 state than in the ground state S_0.

Substitution with an electron-donor ligand generally reduces the IE of the parent molecule by destabilizing the HOMO, whereas the substitution with an electron-withdrawing ligand increases the IE by stabilizing the HOMO. The calculated HOMO and LUMO energies with B3PW91/6311++G(d,p) level of theory are shown in Table 3. In general, CH_3, OH, and OCH_3 are known as electron-donor ligands, whereas F and CN are known as electron-withdrawing ligands. The results show that the substitution with an electron-donor ligand reduces both HOMO and LUMO energies of the parent molecule, whereas the substitution with an electron-withdrawing ligand increases both HOMO and LUMO energies of the parent molecule. The molecular IE is related to its HOMO energy, i.e. in general, the lower the HOMO energy, the higher IE. The ordering of IE of molecules in Table 3 predicted by this rule is in agreement with the measured one except for 2ABN and 4ABN. The measured IE difference between 2ABN and 4ABN is 160 cm^{-1}, which is too small to be resolved by this level of calculations. The CN substituted molecules have much lower HOMOs than the parent molecules, so they have more higher IE, see Table 3. The IEs of 2ABN, 4ABN, 4-cyanophenol and 4-cyanoanisole are 4382, 4222, 4073, and 4010 cm^{-1} larger than their parent molecules, respectively.

4.3. Active vibrations in the S_1 and D_0 states

Table 4 lists several observed vibrational frequencies in D_0 state along with the corresponding ones in the S_1 state for comparison. Evidently, the vibrational frequencies of in-plane modes 15, 6b, 1, 12 in the D_0 state are 7–23 cm^{-1} larger than those in the electronically excited state S_1. This is due to the fact that the molecular geometry is slightly more rigid in the D_0 state than in the S_1 states. Some similar observations have been reported for *m*-methylanisole [29], *p*-methylanisole [30], *m*-cresol [31], *p*-fluorophenol [32], *o*-fluorophenol and *p*-methoxyphenol [33,34]. However, for the vibrational modes 17b and 5 which are related to the out-of-plane bending, the larger differences between the D_0 and S_1 vibration frequencies are found. These facts show that the out-of-plane vibrations of the ring are affected more than the in-plane vibrations of the ring in ionization process. Relative to the aromatic ring, the CN in-plane bending βCN has the opposite effect, i.e. its vibrational frequency in the D_0 state is 134 cm^{-1}, which is 5 cm^{-1} less than that in the S_1 state. This is caused by electron density redistribution in the ionization process. The C-CN bond in the D_0 state is slightly less rigid than that in the S_1 state.

5. Conclusion

Two-color REMPI, PIE and MATI experiments of 2-aminobenzonitrile have been performed to study the vibronic transition and the threshold ionization. Band origin of the $S_1 \leftarrow S_0$ electronic transition appears at 31,265 ± 2 cm^{-1}. The IE of 2-aminobenzonitrile is determined to be 66,653 ± 5 cm^{-1} by the MATI spectroscopy. Analysis on the obtained spectral features shows that most of the active vibrations are related to the in-plane ring deformation in the S_1 and D_0 state. A lot of spectral bands of the excited state S_1 and the cationic ground state D_0 are observed.

We have also performed density functional calculations to obtain structure parameters, total energies, and vibrational frequencies of 2-aminobenzonitrile in the S_0, S_1, and D_0 states. The calculated results give a great aid in the spectral assignment. The CBS-QB3 calculations underestimate the IE by only 0.18%, and the G4 calculations overestimate the IE by 0.47%. These theoretical computations contributed to the corwincing assignments of experimental results.

Acknowledgments

This work was supported by the National Key R&D Program of China (Grant No. 2017YFA0304203), the Chang jiang Scholars and Innovative Research Team in the University of the Ministry of Education of China (Grant No. IRT13076), National Natural Science Foundation of China (Grants Nos. 61378039, 61378049, 61575115, 11434007), the Construction of State Key Laboratory of Quantum Optics and Quantum Optics Devices, China (Grant No. 2015012001-20), and Fund for Shanxi "1331 Project" Key Subjects Construction.

References

[1] L.C.L. Huang, J.L. Lin, W.B. Tzeng, Chem. Phys. 261 (2000) 449.
[2] K. Sakota, N. Yamamoto, K. Ohashi, M. Saeki, S. Ishiuchi, M. Sakai, M. Fujii, Hiroshi Sekiy, Phys. Chem. Chem. Phys. 5 (2003) 1775.
[3] P. Kolek, K. Pirowska, J. Najbar, Phys. Chem. Chem. Phys. 3 (2001) 4874.
[4] G. Varsanyi, S. Szoke, Vibrational Spectra of Benzene Derivatives, Academic Press, New York, 1969.
[5] G. Varsanyi, Assignments of Vibrational Spectra of Seven Hundred Benzene Derivatives, Wiley, New York, 1974.
[6] X. Li, Y. Zhao, Y.H. Jin, X.R. Wang, X.Q. Yu, M. Wu, Y.X. Han, Y.G. Yang, C.Y. Li, S. T. Jia, Acta Phys. Sin. 66 (2017) 093301.
[7] Y.Q. Xu, S.Y. Tzeng, V. Shivatare, K. Takahashi, B. Zhang, W.B. Tzeng, J. Chem. Phys. 142 (2015) 124314.
[8] P.Y. Wu, H.H. Huang, K.C. Lin, W.B. Tzeng, Chem. Phys. Lett. 682 (2017) 34.

[9] M.J. Frisch, G.W. Trucks, H.B. Schlegel, G.E. Scuseria, M.A. Robb, J.R. Cheeseman, G. Scalmani, V. Barone, B. Mennucci, G.A. Petersson, et al., Gaussian 09, Gaussian Inc, Walling-ford CT, 2009.
[10] E.B. Wilson, Phys. Rev. 45 (1934) 706.
[11] J.L. Lin, L.C.L. Huang, W.B. Tzeng, Asian J. Spectrosc. 3 (1999) 115.
[12] W.B. Tzeng, K. Narayanan, G.C. Chang, Appl. Spectrosc. 52 (1998) 890.
[13] W.B. Tzeng, J.L. Lin, K. Narayanan, J. Chem. Soc., Faraday Trans. 94 (1998) 2913.
[14] W.B. Tzeng, K. Narayanan, J. Mol. Struct. 482 (1999) 315.
[15] W.E. Sinclair, D.W. Pratt, J. Chem. Phys. 105 (1996) 7942.
[16] W.B. Tzeng, K. Narayanan, J. Mol. Struct. (Theochem) 434 (1998) 247.
[17] J. Lin, K.C. Lin, W.B. Tzeng, J. Phys. Chem. A 106 (2002) 6462.
[18] S.J. Baek, K.W. Choi, Y.S. Choi, S.K. Kim, J. Chem. Phys. 117 (2002) 2131.
[19] M. Gerhards, S. Schumm, C. Unterberg, K. Kleinermanns, Chem. Phys. Lett. 294 (1998) 65.
[20] J. Lin, J.L. Lin, W.B. Tzeng, Chem. Phys. Lett. 371 (2003) 662.
[21] X. Song, M. Yang, E.R. Davidson, J.P. Reilly, J. Chem. Phys. 99 (1993) 3224.
[22] J. Lin, W.B. Tzeng, J. Chem. Phys. 115 (2001) 743.
[23] O. Dopfer, K. Muller-Dethlefs, J. Chem. Phys. 101 (1999) 8508.
[24] M. Pradhan, C.Y. Li, J.L. Lin, W.B. Tzeng, Chem. Phys. Lett. 407 (2005) 100.
[25] J. Lin, W.B. Tzeng, Phys. Chem. Chem. Phys. 2 (2000) 3759.
[26] J.L. Lin, C.J. Huang, C.H. Lin, W.B. Tzeng, J. Mol. Spec. 244 (2007) 1.
[27] M.C. Capello, M. Broquier, S.I. Ishiuchi, W.Y. Sohn, M. Fujii, C. Dedonder-Lardeux, C. Jouvet, G.A. Pino, J. Phys. Chem. A 118 (2014) 2056.
[28] C.Y. Li, M. Pradhan, W.B. Tzeng, Chem. Phys. Lett. 411 (2005) 506.
[29] Q. Chen, S.Y. Tzeng, B. Zhang, W.B. Tzeng, Acta Phys. Chim. Sin. 30 (2014) 1416.
[30] J.G. Huang, C.Y. Li, W.B. Tzeng, Chem. Phys. Lett. 414 (2005) 276.
[31] J.G. Huang, J.L. Lin, W.B. Tzeng, Spectrochimica Acta Part A 67 (2007) 989.
[32] B. Zhang, C.Y. Li, H.W. Su, J.L. Lin, W.B. Tzeng, Chem. Phys. Lett. 390 (2004) 65.
[33] C.Y. Li, H.W. Su, W.B. Tzeng, Chem. Phys. Lett. 410 (2005) 99.
[34] L.W. Yuan, C.Y. Li, J.L. Lin, S.C. Yang, Wen Bih Tzeng, Chem. Phys. 323 (2006) 429.